

Numerical solutions and stability analysis of unsteady hybrid nanofluid flow over a shrinking sheet with heat generation

Rahman N. A.¹, Khashi'ie N. S.^{2,3}, Hamzah K. B.^{2,3}, Waini I.^{2,3}, Rosli M. A. M.¹, Pop I.⁴

¹*Fakulti Kejuruteraan Mekanikal, Universiti Teknikal Malaysia Melaka, Hang Tuah Jaya, 76100 Durian Tunggal, Melaka, Malaysia*

²*Fakulti Teknologi Kejuruteraan Mekanikal dan Pembuatan, Universiti Teknikal Malaysia Melaka, Hang Tuah Jaya, 76100 Durian Tunggal, Melaka, Malaysia*

³*Forecasting and Engineering Technology Analysis (FETA) Research Group, Universiti Teknikal Malaysia Melaka, Hang Tuah Jaya, 76100 Durian Tunggal, Melaka, Malaysia*

⁴*Department of Mathematics, Babes-Bolyai University, R-400084 Cluj-Napoca, Romania*

(Received 26 September 2023; Accepted 7 November 2023)

The study focuses on the generation of multiple numerical solutions and stability analysis for the case of an unsteady copper-alumina/water hybrid nanofluid subjected to a shrinking sheet. Heat generation as the potential contributing factor in the heat transfer progress is considered as well as the suction effect. The governing model (partial differential equations) is developed based on the boundary layer assumptions, which then are transformed into a set of ordinary (similarity) differential equations. The *bvp4c* solver is used to search all possible solutions and conduct the stability analysis for the generating solutions. Suction induces the movement of heated fluid particles towards the wall, resulting in increased velocity and heat transfer and a decrease in temperature. The first solution is proved to be the stable real solution as compared to the other solution.

Keywords: *hybrid nanofluid; heat generation; heat transfer; multiple solutions; unsteady flow.*

2010 MSC: 76W05,76A10

DOI: 10.23939/mmc2023.04.1222

1. Introduction

The advancement in nanotechnology has led to the creation of a subcategory class called hybrid nanofluid prepared by the dispersion of two nanoparticles into a base/working fluid with addition of additives to aid the dispersion process. The greater stability is achieved in conjunction with the surface modification and strong cluster bonds between the nanoparticles. Various studies have been conducted to show the properties of hybrid nanofluids in other instances and experiments. Duangthongsuk and Wongwises [1] used TiO_2 /water hybrid nanofluid to obtain thermal conductivity with temperature constraints. On the other hand, Sheikholeslami and Sadoughi [2] studied the impact of heat transfer when CuO /water nanofluid is experiencing magnetic field disruptions where the convective performance is seen to have reduced. The application of nanofluids can be observed in food industries as Jacobsen et al. [3] wrote about spray dyeing using electrohydrodynamic (EHD). Further references that highlighted the applications of nanofluids are in [4–9].

In an unsteady flow, it is seen that the amount of liquid flowing per second is not at a constant rate. There have been several studies that have touched on this factor and one of the research projects was done by Sreedevi et al. [10], where the unsteady magnetohydrodynamic heat and mass transfer was analysed for the combination of carbon nanotubes and silver nanoparticles interacting with suction

The grant FRGS/1/2021/STG06/UTEM/03/1 from Universiti Teknikal Malaysia Melaka and Ministry of Higher Education (Malaysia) is acknowledged.

and having slip effects due to chemical reactions. Khan et al. [11] proposed research on the heat transfer of hybrid nanofluid Cu-Al₂O₃/water passing through a radially shrinking and stretching surface. Meanwhile, Waini et al. [12] studied the unsteady flow of the same hybrid nanofluid on a stagnation point over a permeable rigid surface. Moreover, Zainal et al. [13] focused on the unsteady electro-magnetohydrodynamic (EMHD) flow with the application of boundary layer theory over a stretching and shrinking plate for hybrid nanofluid Cu-Al₂O₃/water. Zainal et al. [14] progressed the study with another paper on the three-dimensional stagnation point unsteady MHD convection flow for the same hybrid nanofluid. Another notable mention piece of research was done by Khan et al. [15] using the hybrid nanofluid CNTs-Fe₃O₄/water to study the flow pattern between two parallel plates undergoing a variable magnetic field.

Heat generation is a crucial part in the heat transfer performance of hybrid nanofluids. A lot of studies have emerged in the investigation of the relationship between heat generation and hybrid nanoparticles. Jusoh et al. [16] addressed the impacts of heat transfer of nanofluids including MHD properties and heat generation. Joshi et al. [17] investigated the impact of magnetohydrodynamic (MHD) flow on a bidirectional porous stretchable sheet experiencing volumetric heat generation using the hybrid nanofluid SWCNT+Ag+water. Wahid et al. [18] analyzed the hybrid nanofluid flow with heat generation and slip effects subjected to an exponentially stretching/shrinking sheet. With all the research that has been studied, huge inspiration has been struck on solving the unsteady flow with heat generation focusing on hybrid nanofluid and subsequently, filling up the knowledge gaps on this subject matter. In this paper, the hybrid nanofluid from copper-alumina/water will be studied focusing on the unsteady flow with the suction and heat generation effects. The flow is analyzed by considering a permeable stretching/shrinking sheet. The `bvp4c` solver in MATLAB is used to find the solutions for the ordinary differential equations. In the event of the dual visible solutions, stability analysis will be used to determine the stable outcome. With rigorous research done, the author can say for certain this publication has yet to be viewed by other scholars.

2. Mathematical formulation

Consider a hybrid nanofluid with unsteady flow (copper-alumina/water) past a shrinking/stretching sheet. The boundary layer and energy equations are modeled based on the physical assumptions:

- The velocity of the deformable sheet is represented by $u_w = \frac{cx}{1-\alpha t}$ such that t refers to time, α is the representative for the unsteady flow such that $\alpha < 0$ decelerates the outer flow, $\alpha = 0$ for the steady flow and $\alpha > 0$ expedites the flow (see Waini et al. [19]).
- T_w and T_∞ represent the surface and far-field temperatures, respectively.
- The imposed heat generation effect is mathematically expressed as $Q_1 = \frac{Q_0x}{1-\alpha t}$, where Q_1 and Q_0 is the heat generation factor and constant, respectively (see Kumbhakar and Nandi [20]).

Hence, the mathematical model in a two-dimensional system which renders this physical problem are given as [19, 20]

$$\frac{\partial u}{\partial x} + \frac{\partial v}{\partial y} = 0, \tag{1}$$

$$\frac{\partial u}{\partial t} + u \frac{\partial u}{\partial x} + v \frac{\partial u}{\partial y} = \frac{\mu_{hnf}}{\rho_{hnf}} \frac{\partial^2 u}{\partial y^2}, \tag{2}$$

$$\frac{\partial T}{\partial t} + u \frac{\partial T}{\partial x} + v \frac{\partial T}{\partial y} = \frac{k_{hnf}}{(\rho C_p)_{hnf}} \frac{\partial^2 T}{\partial y^2} + \frac{Q_1}{(\rho C_p)_{hnf}} (T - T_\infty), \tag{3}$$

$$\begin{cases} u = \lambda u_w, & v = v_w, & T = T_w & \text{when } y = 0, \\ u \rightarrow 0, & v \rightarrow 0, & T \rightarrow T_\infty & \text{as } y \rightarrow \infty, \end{cases} \tag{4}$$

By considering u, v as the velocities of hybrid nanofluid and T as the temperature, the similarity transformation is given by

$$\eta = \sqrt{\frac{c}{\nu_f}} \frac{y}{1 - \alpha t}, \quad u = \frac{cx}{1 - \alpha t} f'(\eta), \quad v = -\sqrt{\frac{c\nu_f}{1 - \alpha t}} f(\eta), \quad \theta(\eta) = \frac{T - T_\infty}{T_w - T_\infty}. \tag{5}$$

Equation (5) is substituted into Eqs. (2)–(4) to form a set of similarity ordinary differential equations (ODEs) [19,20]

$$\left(\frac{\mu_{hnf}/\mu_f}{\rho_{hnf}/\rho_f}\right) f''' - (f')^2 + ff'' - S(f' + 0.5\eta f'') = 0, \tag{6}$$

$$\frac{1}{Pr} \frac{k_{hnf}/k_f}{(\rho C_p)_{hnf}/(\rho C_p)_f} \theta'' - (0.5S\eta - f)\theta' + \frac{Q}{(\rho C_p)_{hnf}/(\rho C_p)_f} \theta = 0, \tag{7}$$

$$f(0) = B, \quad f'(0) = \lambda, \quad \theta(0) = 1, \quad f'(\eta) \rightarrow 0, \quad \theta(\eta) \rightarrow 0, \tag{8}$$

where the parameters in Eqs. (6)–(8) are defined as:

- unsteadiness parameter ($S = \alpha/c$); $S > 0$ for unsteadiness accelerating flow, $S < 0$ for unsteadiness decelerating flow and $S = 0$ for the steady flow case;
- stretching/shrinking parameter λ ; $\lambda < 0$ for the shrinking case, $\lambda = 0$ for the static sheet and $\lambda > 0$ for the stretching case;
- mass flux parameter B , $B < 0$ for the injection process, $B = 0$ for the impermeable surface and $B > 0$ for the suction process;
- heat generation parameter ($Q = \frac{Q_0}{c(\rho C_p)_f}$), $Q < 0$ for the heat absorption process and $Q > 0$ for the heat generation process, and
- Prandtl number ($Pr = (\mu C_p)_f/k_f$).

Table 1. General correlations of hybrid nanofluid.

Properties	Correlations
Thermal Conductivity	$k_{hnf} = \left[\frac{\left(\frac{\phi_1 k_1 + \phi_2 k_2}{\phi_{hnf}}\right) - 2\phi_{hnf} k_f + 2(\phi_1 k_1 + \phi_2 k_2) + 2k_f}{\left(\frac{\phi_1 k_1 + \phi_2 k_2}{\phi_{hnf}}\right) + \phi_{hnf} k_f - (\phi_1 k_1 + \phi_2 k_2) + 2k_f} \right] k_f$
Heat Capacity	$(\rho C_p)_{hnf} = (\rho C_p)_{s1} \phi_1 + (\rho C_p)_{s2} \phi_2 + (1 - \phi_{hnf})(\rho C_p)_f$
Density	$\rho_{hnf} = \rho_{s1} \phi_1 + \rho_{s2} \phi_2 + (1 - \phi_{hnf})\rho_f$
Dynamic Viscosity	$\mu_{hnf} = \mu_f / (1 - \phi_{hnf})^{2.5}$; $\phi_{hnf} = \phi_1 + \phi_2$

Table 2. Properties of the water and nanoparticles.

Properties	Water base fluid	Copper	Alumina
ρ (kg/m ³)	997.1	8933	3970
C_p (J/kg K)	4179	385	765
k (W/m K)	0.613	400	40
Prandtl number	6.2		

Tables 1 and 2 display the experimentally validated correlations of properties for hybrid nanofluids and properties for the copper, graphene and water (see Takabi and Salehi [21] and Oztop and Abu-Nada [22]).

The definition of skin friction and local Nusselt number are

$$C_f = \frac{\mu_{hnf}}{\rho_f u_w^2} \left(\frac{\partial u}{\partial y}\right)_{y=0}, \quad Nu_x = -\frac{x k_{hnf}}{k_f (T_w - T_\infty)} \left(\frac{\partial T}{\partial y}\right)_{y=0}. \tag{9}$$

Substituting Eq. (5) into Eq. (9),

$$Re_x^{1/2} C_f = \frac{\mu_{hnf}}{\mu_f} f''(0), \quad Re_x^{-1/2} Nu_x = \frac{-k_{hnf}}{k_f} \theta'(0), \tag{10}$$

where the local Reynolds number is $Re_x = \frac{x u_w}{\nu_f}$.

3. Stability analysis

The significance of this process lies in its role in identifying the actual solution from a pool of possible solutions. Building upon the initial research into stability analysis, the subsequent transformation is examined:

$$\eta = \sqrt{\frac{c}{\nu_f}} \frac{y}{1 - \alpha t}, \quad u = \frac{cx}{1 - \alpha t} \frac{\partial f(\eta, \tau)}{\partial \eta}, \quad v = -\sqrt{\frac{c\nu_f}{1 - \alpha t}} f(\eta, \tau), \quad \theta(\eta, \tau) = \frac{T - T_\infty}{T_w - T_\infty}, \quad \tau = \frac{ct}{1 - \alpha t}. \quad (11)$$

The obtained differential equations upon the substitution of Eq. (11) into Eqs. (2)–(4) are

$$\left(\frac{\mu_{hnf}/\mu_f}{\rho_{hnf}/\rho_f}\right) \frac{\partial^3 f}{\partial \eta^3} - \left(\frac{\partial f}{\partial \eta}\right)^2 + f \frac{\partial^2 f}{\partial \eta^2} - S \left(\frac{\partial f}{\partial \eta} + 0.5\eta \frac{\partial^2 f}{\partial \eta^2}\right) - \frac{\partial^2 f}{\partial \eta \partial \tau} = 0, \quad (12)$$

$$\frac{1}{Pr} \frac{k_{hnf}/k_f}{(\rho C_p)_{hnf}/(\rho C_p)_f} \frac{\partial^2 \theta}{\partial \eta^2} - (0.5S\eta - f) \frac{\partial \theta}{\partial \eta} + \frac{Q}{(\rho C_p)_{hnf}/(\rho C_p)_f} \theta - \frac{\partial \theta}{\partial \eta} = 0, \quad (13)$$

$$f(0, \tau) = B, \quad \frac{\partial f}{\partial \eta}(0, \tau) = \lambda, \quad \theta(0, \tau) = 1, \quad \frac{\partial f}{\partial \eta}(\infty, \tau) \rightarrow 0, \quad \theta(\infty, \tau) \rightarrow 0, \quad (14)$$

Equation (15) is the perturbation function which is used to identify the disturbance in the similarity solutions. The function F and G are related to f_0 and θ_0 , respectively while γ is the eigenvalue,

$$f(\eta, \tau) = f_0(\eta) + e^{-\gamma t} F(\eta), \quad \theta(\eta, \tau) = \theta_0(\eta) + e^{-\gamma t} G(\eta). \quad (15)$$

The final form of eigenvalue equations by considering the relaxing conditions to prevent homogeneous eigenvalues solution are:

$$\left(\frac{\mu_{hnf}/\mu_f}{\rho_{hnf}/\rho_f}\right) F''' - 2f_0' F' + f_0 F'' + F f_0'' - S(F' + 0.5\eta F'') + \gamma F = 0, \quad (16)$$

$$\frac{1}{Pr} \frac{k_{hnf}/k_f}{(\rho C_p)_{hnf}/(\rho C_p)_f} G'' - (0.5S\eta - f_0) G' + F \theta_0' + \gamma G + \frac{Q}{(\rho C_p)_{hnf}/(\rho C_p)_f} G = 0, \quad (17)$$

$$F(0) = 0, \quad F'(0) = 0, \quad F''(0) = 1 \quad (\text{added}) \quad G(0) = 0, \quad F'(\eta) \rightarrow 0 \quad (\text{relaxed}), \quad G(\eta) \rightarrow 0. \quad (18)$$

These linearized equations are obtained by substituting Eq. (15) into Eqs. (12)–(14).

4. Numerical results and discussion

The `bvp4c` solver in the Matlab software is a potent tool for computing nonlinear ODEs. The numerical solutions are obtained by computing Eqs. (6)–(8) using the properties given in Tables 1 and 2. The validation of the present model is presented in Tables 3 and 4, respectively and is in good agreement with previous study which affirms the calculations validity. From these tables, it also can be highlighted that as the unsteadiness parameter reduces from $S = 0$ to $S = -5$, the values of $Re_x^{1/2} C_f$ reduces while $Re_x^{-1/2} Nu_x$ increases. The explanations of the flow and thermal behaviors for copper-alumina/water are then, discussed and presented for the variation of suction parameter B and stretching/shrinking parameter λ . Others are set as follows: $Pr = 6.2$ (water), $S = -1$, $Q = 0.02$ and $\phi_1 = \phi_2 = 0.01$.

Table 3. Validation of $Re_x^{1/2} C_f$ when $\phi_1 = 0.2$ (copper), $\phi_2 = 0$ (alumina), $Q = 0$, $B = 2.1$, $\lambda = -1$ and various S .

S	Present		Waini et al. [19]	
	First Solution	Second Solution	First Solution	Second Solution
0	2.528970	0.586548	2.528984	0.584729
-0.2	2.462145	-0.048071	2.462145	-0.048071
-0.4	2.395251	-0.473472	2.395252	-0.473472
-0.6	2.328304	-0.840776	2.328304	-0.840776
-1	2.194247	-1.491281	2.194247	-1.491281
-3	1.521192	-4.144746	1.521197	-4.144746
-5	0.844435	-6.431507	0.844435	-6.431507

Table 4. Validation of $Re_x^{-1/2}Nu_x$ when $\phi_1 = 0.2$ (copper), $\phi_2 = 0$ (alumina), $Q = 0$, $B = 2.1$, $\lambda = -1$ and various S .

S	Present		Waini et al. [19]	
	First Solution	Second Solution	First Solution	Second Solution
0	6.822453	6.693244	6.822454	6.693105
-0.2	6.875796	6.716536	6.875796	6.716536
-0.4	6.927417	6.755470	6.927417	6.755470
-0.6	6.977507	6.797695	6.977507	6.797695
-1	7.073680	6.884548	7.073680	6.884548
-3	7.497151	7.296176	7.497151	7.296176
-5	7.858446	7.657801	7.858446	7.657801

The graphical results for the skin friction, $Re_x^{1/2}C_f$ and local Nusselt number, $Re_x^{-1/2}Nu_x$ with various S and λ are presented in Figures 1 and 2, respectively. There exist dual solutions for each value of λ when $B = 3, 3.1, 3.2$. The critical values λ_c are clearly presented in these figures. It is apparent that the critical values increase ($\lambda_c = -2.2745, -2.4336, -2.5982$) as B increases which implies the success of suction effect in delaying the boundary layer separation. The suction parameter is seen to enhance the values of $Re_x^{1/2}C_f$ as well as $Re_x^{-1/2}Nu_x$ of the hybrid copper-alumina/water nanofluid. The physical explanation is the suction induces the movement of heated fluid particles towards the wall, resulting in the increment of skin friction coefficient, velocity as well and heat transfer with a decrease in temperature (see Figures 3 and 4).

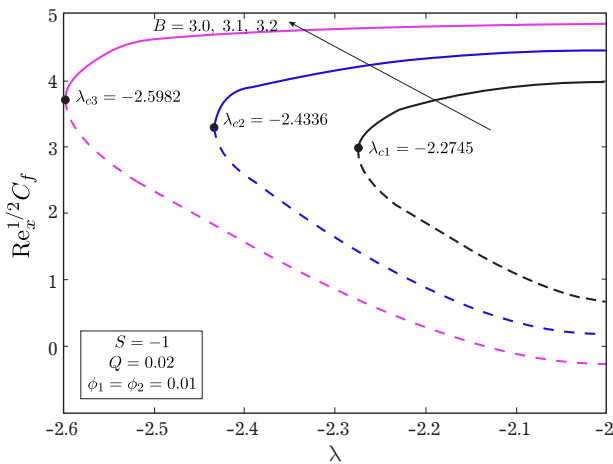


Fig. 1. $Re_x^{1/2}C_f$ for various B .

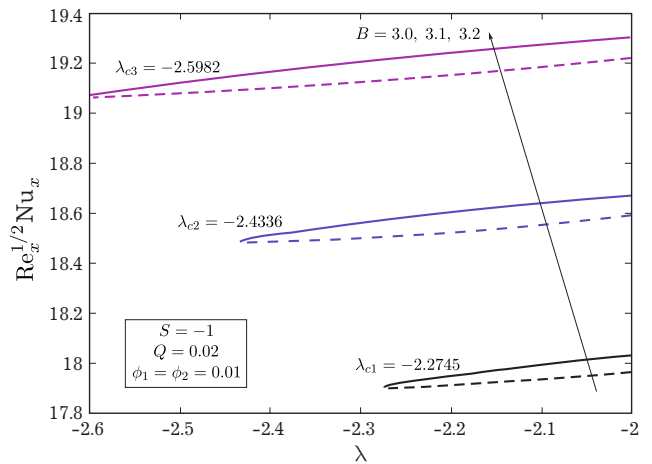


Fig. 2. $Re_x^{-1/2}Nu_x$ for various B .

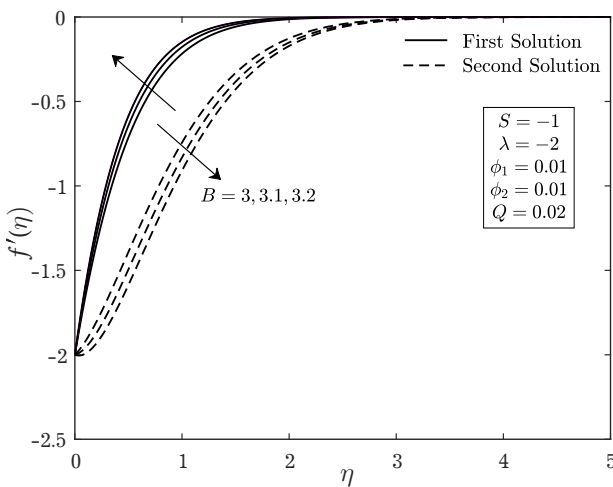


Fig. 3. Velocity profile for various B .

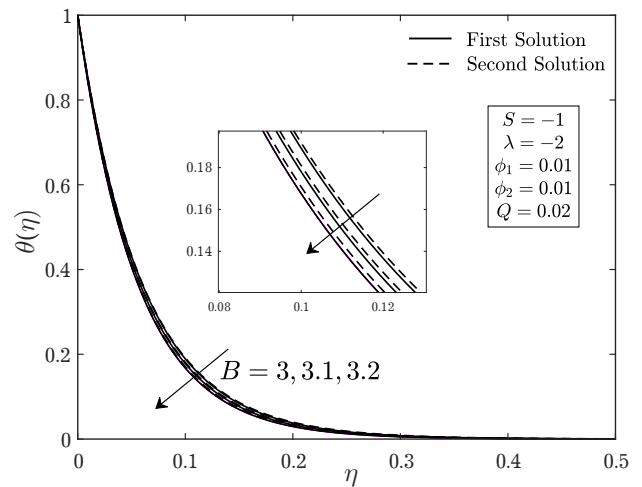


Fig. 4. Temperature profile for various B .

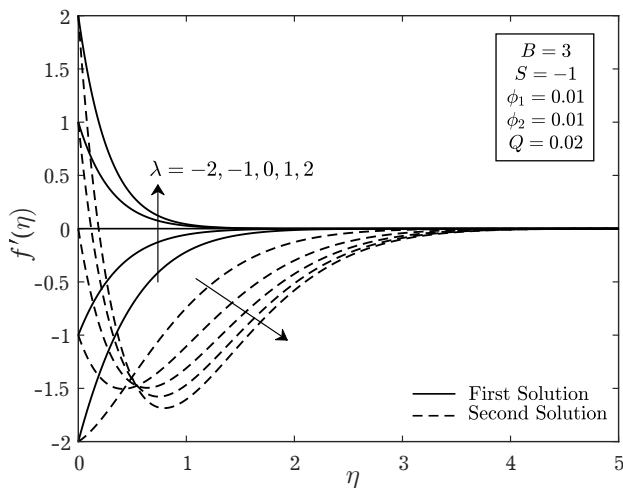


Fig. 5. Velocity profile for various λ .

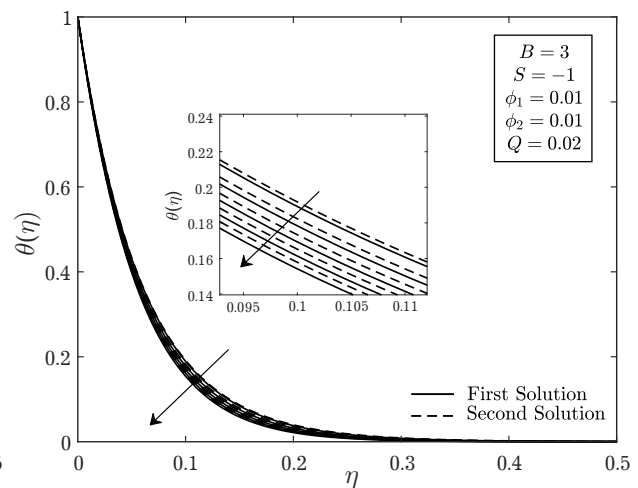


Fig. 6. Temperature profile for various λ .

All the profiles in Figures 3 to 6 fulfill the boundary condition in Eq. (8) which implies the legitimate model. Further, the velocity distribution (first solution) in Figure 5 expands with the increment of λ but the temperature distribution (Figure 6) shows an adverse result. The addition of the stretching/shrinking parameter implies the incremental strength of assisting flow in the generation of boundary layer solutions. Meanwhile, Figure 7 displays the result of stability analysis showing the smallest eigenvalues γ_1 approaching 0 as the values of λ moves to the selected critical value. This affirms the reliability of the stability analysis formulation and in addition, the first solution is stable based on the positive values of the smallest eigenvalues.

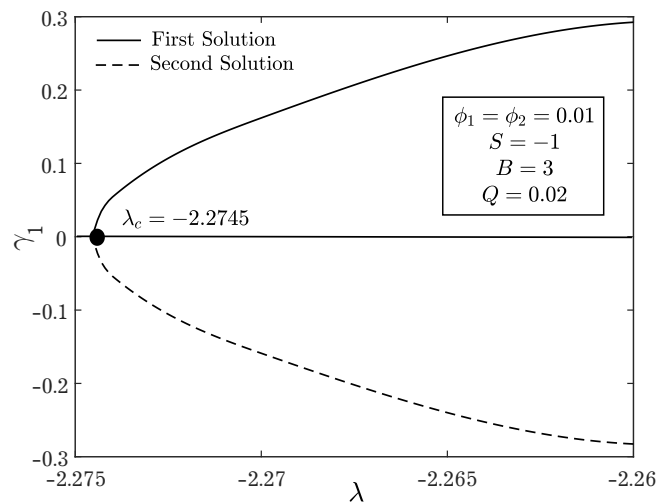


Fig. 7. Stability analysis.

5. Conclusions

The case of hybrid nanofluid with unsteady flow past a deformable sheet with heat generation has several conclusions as follow:

- Dual solutions are achievable at the shrinking and stretching surfaces.
- Stability analysis proves that only one solution (first solution) is stable.
- The addition of suction and stretching/shrinking ($\lambda \rightarrow +\lambda$) parameters gives similar trend on the velocity and temperature distributions where the velocity profile increases while the temperature decreases.
- The addition of suction delays the separation process by enlarging the critical value. Besides, suction also helps the fluid motion by increasing the skin friction as well as the thermal progress.

[1] Duangthongsuk W., Wongwises S. Measurement of temperature-dependent thermal conductivity and viscosity of TiO₂-water nanofluids. *Experimental Thermal and Fluid Science*. **33** (4), 706–714 (2009).
 [2] Sheikholeslami M., Sadoughi M. K. Simulation of CuO-water nanofluid heat transfer enhancement in presence of melting surface. *International Journal of Heat and Mass Transfer*. **116**, 909–919 (2018).

- [3] Jacobsen C., García-Moreno P. J., Mendes A. C., Mateiu R. V., Chronakis I. S. Use of electrohydrodynamic processing for encapsulation of sensitive bioactive compounds and applications in food. *Annual Review of Food Science and Technology*. **9** (1), 525–549 (2018).
- [4] Minea A. A., El-Maghlany W. M. Influence of hybrid nanofluids on the performance of parabolic trough collectors in solar thermal systems: Recent findings and numerical comparison. *Renewable Energy*. **120**, 350–364 (2018).
- [5] Aglawe K. R., Yadav R. K., Thool S. B. Preparation, applications and challenges of nanofluids in electronic cooling: A systematic review. *Materials Today: Proceedings*. **43** (1), 366–372 (2021).
- [6] Hafeez M. B., Amin R., Nisar K. S., Jamshed W., Abdel-Aty A. H., Khashan M. M. Heat transfer enhancement through nanofluids with applications in automobile radiator. *Case Studies in Thermal Engineering*. **27**, 101192 (2021).
- [7] Kumar V., Sarkar J., Yan W. M. Thermal-hydraulic behavior of lotus like structured rGO-ZnO composite dispersed hybrid nanofluid in mini channel heat sink. *International Journal of Thermal Sciences*. **164**, 106886 (2021).
- [8] Gawusu S., Zhang X. Hydrodynamics analysis of Taylor flow in oil and gas pipelines under constant heat flux. *Heat and Mass Transfer*. **57** (3), 515–527 (2021).
- [9] Anandika R., Puneeth V., Manjunatha S., Chamkha A. J. Thermal optimisation through multilayer convective flow of CuO-MWCNT hybrid nanofluid in a composite porous annulus. *International Journal of Ambient Energy*. **43** (1), 6463–6473 (2022).
- [10] Sreedevi P., Sudarsana Reddy P., Chamkha A. Heat and mass transfer analysis of unsteady hybrid nanofluid flow over a stretching sheet with thermal radiation. *SN Applied Sciences*. **2** (7), 1222 (2020).
- [11] Khan U., Waini I., Ishak A., Pop I. Unsteady hybrid nanofluid flow over a radially permeable shrinking/stretching surface. *Journal of Molecular Liquids*. **331**, 115752 (2021).
- [12] Waini I., Ishak A., Pop I. Unsteady hybrid nanofluid flow on a stagnation point of a permeable rigid surface. *ZAMM – Journal of Applied Mathematics and Mechanics / Zeitschrift für Angewandte Mathematik und Mechanik*. **101** (6), e202000193 (2021).
- [13] Zainal N. A., Nazar R., Naganthran K., Pop I. Unsteady EMHD stagnation point flow over a stretching/shrinking sheet in a hybrid $\text{Al}_2\text{O}_3\text{-Cu}/\text{H}_2\text{O}$ nanofluid. *International Communications in Heat and Mass Transfer*. **123**, 105205 (2021).
- [14] Zainal N. A., Nazar R., Naganthran K., Pop I. Unsteady MHD Mixed Convection Flow in Hybrid Nanofluid at Three-Dimensional Stagnation Point. *Mathematics*. **9** (5), 549 (2021).
- [15] Khan M. S., Mei S., Fernandez-Gamiz U., Noeiaghdam S., Shah S. A., Khan A. Numerical analysis of unsteady hybrid nanofluid flow comprising CNTs-ferrous oxide/water with variable magnetic field. *Nanomaterials*. **12** (2), 180 (2022).
- [16] Jusoh R., Nazar R., Pop I. Impact of heat generation/absorption on the unsteady magnetohydrodynamic stagnation point flow and heat transfer of nanofluids. *International Journal of Numerical Methods for Heat & Fluid Flow*. **30** (2), 557–574 (2020).
- [17] Joshi N., Upreti H., Pandey A. K., Kumar M. Heat and mass transfer assessment of magnetic hybrid nanofluid flow via bidirectional porous surface with volumetric heat generation. *International Journal of Applied and Computational Mathematics*. **7** (3), 64 (2021).
- [18] Wahid N. S., Arifin N. M., Khashi'ie N. S., Pop I. Hybrid nanofluid slip flow over an exponentially stretching/shrinking permeable sheet with heat generation. *Mathematics*. **9** (1), 30 (2020).
- [19] Waini I., Ishak A., Pop I. Unsteady flow and heat transfer past a stretching/shrinking sheet in a hybrid nanofluid. *International Journal of Heat and Mass Transfer*. **136**, 288–297 (2019).
- [20] Kumbhakar B., Nandi S. Unsteady MHD radiative-dissipative flow of $\text{Cu-Al}_2\text{O}_3/\text{H}_2\text{O}$ hybrid nanofluid past a stretching sheet with slip and convective conditions: A regression analysis. *Mathematics and Computers in Simulation*. **194**, 563–587 (2019).
- [21] Takabi B., Salehi S. Augmentation of the heat transfer performance of a sinusoidal corrugated enclosure by employing hybrid nanofluid. *Advances in Mechanical Engineering*. **6**, 147059 (2014).
- [22] Oztop H. F., Abu-Nada E. Numerical study of natural convection in partially heated rectangular enclosures filled with nanofluids. *International journal of heat and fluid flow*. **29** (5), 1326–1336 (2008).

Чисельні розв'язки та аналіз стійкості нестационарного гібридного потоку нанорідини по листу, що стискається, із виділенням тепла

Рахман Н. А.¹, Хашііє Н. С.^{2,3}, Хамза К. Б.^{2,3}, Вайні І.^{2,3}, Рослі М. А. М.¹, Поп І.⁴

¹Факультет машинобудування Технічного університету Малайзії в Мелаці,

Ханг Туах Джая, 76100 Дуріан Тунггал, Малакка, Малайзія

²Факультет машинобудування та технологій виробництва, Технічний університет Малайзії, Малака,

Ханг Туах Джая, 76100 Дуріан Тунггал, Малакка, Малайзія

³Дослідницька група прогнозування та аналізу інженерних технологій (FETA),

Технічний університет Малайзії Малакка,

Ханг Туах Джая, 76100 Дуріан Тунггал, Малака, Малайзія

⁴Факультет математики, Університет Бабеш-Бойяї,

R-400084 Клуж-Напока, Румунія

Дослідження зосереджено на створенні декількох чисельних розв'язків і аналізі стійкості для випадку нестационарної гібридної нанорідини мідь-глинозем/вода на листі, що стискається. Розглядаються ефект всмоктування та виділення тепла як потенційні фактори, що сприяють прогресу теплопередачі. Вихідна модель, а саме рівняння в частинних похідних розроблені на основі припущень про граничний шар, які потім перетворюються на набір звичайних (подібних) диференціальних рівнянь. Розв'язувач `bvp4c` використовується для пошуку всіх можливих розв'язків і проведення аналізу стійкості для розв'язків, які генеруються. Всмоктування викликає рух нагрітих частинок рідини до стінки, що призводить до збільшення швидкості та теплопередачі, а також до зниження температури. Доведено, що перший розв'язок є стійким дійсним розв'язком порівняно з іншим розв'язком.

Ключові слова: *гібридна нанорідина; виділення тепла; теплопередача; множинні розв'язки; нестационарний потік.*